Supporting information

Improving Pd-C Catalysts *via* Heteroatom Doping for the Dehydrogenation of Formic Acid: A Non-Noble Metal Modulation Strategy

1. Chemicals

All chemicals were commercially available and used without further purification. Ketjenblack (KB, EC-600JD, Japanese lion), potassium tetrachloropalladite (K_2PdCl_4, Shanghai Macklin Biochemical industry Park, Shanghai, China, >32.6%), nickel (II) nitrate hexahydrate ($Ni(NO_3)_2·6H_2O$, Sinopharm Chemical Reagent Co., Ltd. >98.0%), iron (III) nitrate nonahydrate ($Fe(NO_3)_3·9H_2O$, Sinopharm Chemical Reagent Co., Ltd. >98.5%), cobalt chloride hexahydrate ($CoCl_2·6H_2O$, Shanghai Macklin Biochemical Co., Ltd. AR), manganese(II) nitrate tetrahydrate ($MnN_2O_6·4H_2O$, Shanghai Aladdin Biochemical Technology Co., Ltd. >98%), formic acid (CH_2O_2, Sinopharm Chemical Reagent Co., Ltd. >98%), sodium borohyride ($NaBH_4$, Sinopharm Chemical Reagent Co., Ltd. >98%), L-arginine ($C_6H_{14}N_4O_2$, Shanghai Macklin Biochemical Co., Ltd. >98%), and sodium formate ($CHNaO_2$, Shanghai Aladdin Biochemical Technology Co., Ltd. >99.5%), were used as received. De-ionized (DI) water was obtained by a reverse osmosis followed by the ion-exchange and filtration.

2. Instrumentation and methods

Powder X-ray diffraction patterns were collected on a D8 ADVANCE with Cu-Kα radiation (40 kV 40 mA). N_2 adsorption/desorption isotherms were obtained at 77 K using automatic volumetric adsorption equipment (NOVA3000e). The metal contents of the catalyst were analyzed by an inductively coupled plasma optical emission spectroscopy (ICP-OES) on Thermo Fisher iCAP PRO (OES). X-ray photoelectron spectroscopic (XPS) spectra were recorded on a Thermo Scientific ESCALAB Xi+ using Al Kα source. The transmission electron microscopic (TEM) and high-annular dark-field scanning TEM (HAADF-STEM) images were collected on FEI Talos F200x with the operating voltage at 200 kV. Elemental analyses were performed on Elementar Unicube instruments. Fourier Transform Infrared Spectrometer (FT-IR) analyses were carried out on a Nicolet 380 in air mode. Gas Chromatography (GC) results were analyzed by a FULI 9790 II

instrument with N_2 as the carrier gas.

3. Syntheses

3.1.1 Synthesis of Pd_xNi_y/KB_{LA}: Taking $Pd_{0.95}Ni_{0.05}/KB_{LA}$ as an example, an aqueous mixture containing 1.74 mL of LA (0.1 g mL^{-1}), 0.285 mL of K_2PdCl_4 (0.1 M) and 0.15 mL of $Ni(NO_3)_2 \cdot 6H_2O$ (0.01 M) were firstly diluted to 10 mL with water and sonicated for 5 min. Then, 30 mg of KB carbon was added and sonicated for 10 min to get a homogeneous mixture. This mixture was then stirred at room temperature overnight. Subsequently, 1.0 mL of freshly prepared $NaBH_4$ solution (1.32 M) was injected into the above mixture and stirred at room temperature for another 90 min. Finally, the solid was collected by centrifugation, washed with water for three times, and directly used as the catalysts for formic acid dehydrogenation.

Keeping the total metal amount at 0.03 mmol, other Pd_xNi_y/KB_{LA} with different ratios of metals were prepared by a similar process, except for the usage of metals (the x and y instead for the molar percentage of Pd and Ni, respectively).

To study the effects of supports and surface modifier, control samples with different usage of KB and LA have also been synthesized.

3.1.2 Synthesis of $Pd_{0.95}M_{0.05}/KB_{LA}$ (M = Co, Mn, Fe): The synthesis process was the same as $Pd_{0.95}Ni_{0.05}/KB_{LA}$, except for the use of other metal salts ($Fe(NO_3)_3 \cdot 9H_2O$, $CoCl_2 \cdot 6H_2O$, $MnN_2O_6 \cdot 4H_2O$) in place of $Ni(NO_3)_2 \cdot 6H_2O$ during the catalyst preparation.

4. Measurements for catalytic performance

4.1 Procedure for FA dehydrogenation

In general, 2.0 mL dispersion of as-prepared catalyst in water was placed in 30 mL two-necked round-bottom flask which was placed in a water bath at the preset temperature (30, 40, 50, and 60 °C). A SQB Wet-Gas flow meter was connected to the reaction flask to measure the volume of released gas. The reaction started when 1.0 mL of mixed aqueous solution containing FA (3 M) and SF of different molar ratios (0, 3, 6, and 7.5 M) was injected into the mixture using a syringe. The molar ratio of n_{Ni+Pd}/n_{FA} was theoretically fixed at 0.01 for all catalytic reactions except for the notes in the manuscript. The volume of the evolved gas was monitored by the Wet-Gas flow meter automatically.

3.2.2 Durability testing of $Pd_{0.95}Ni_{0.05}/KB_{LA}$

The durability testing for $Pd_{0.95}Ni_{0.05}/KB_{LA}$ was performed at 50 ℃. The testing process was the same as the description in **3.2.1**. After each cycle, the catalyst was washed by DI-water for 3 times and reused for the next cycle.

4.3 Calculation methods

The turnover frequency (TOF) reported here is an apparent TOF value based on the number of metal atoms (Pd+Ni) in catalysts, which is calculated from the equation as follow:

$$TOF = P_0V/(2RTtn_M)$$

Where P_0 is the atmospheric pressure (101325 Pa), V is the final generated volume of gas (H_2+CO_2), R is the universal gas constant (8.3145 m^3 Pa mol^{-1} K^{-1}), T is the room temperature (298 K), t is the completion time of the reaction in hour, and n_M is the total number of metal atoms (Pd+Ni) in catalysts.

5. Figures and tables

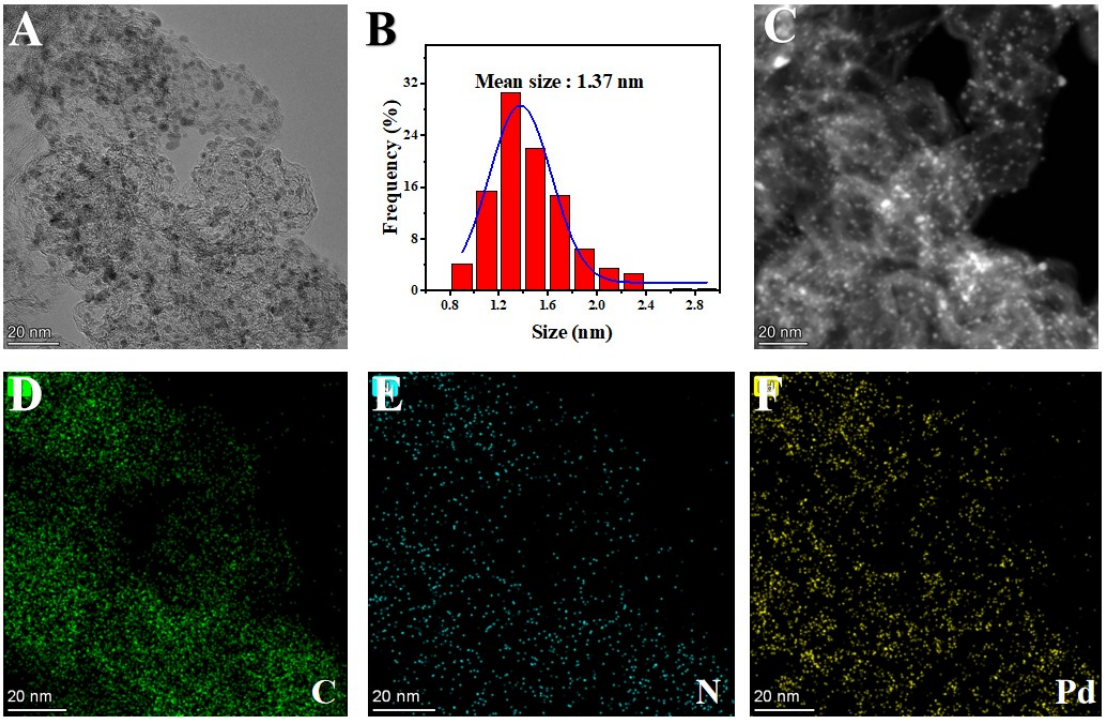

Figure S1. The TEM (A), particle size distribution (B), HADDF-STEM (C), corresponding element mapping (D-F) images of Pd/KB_{LA}.

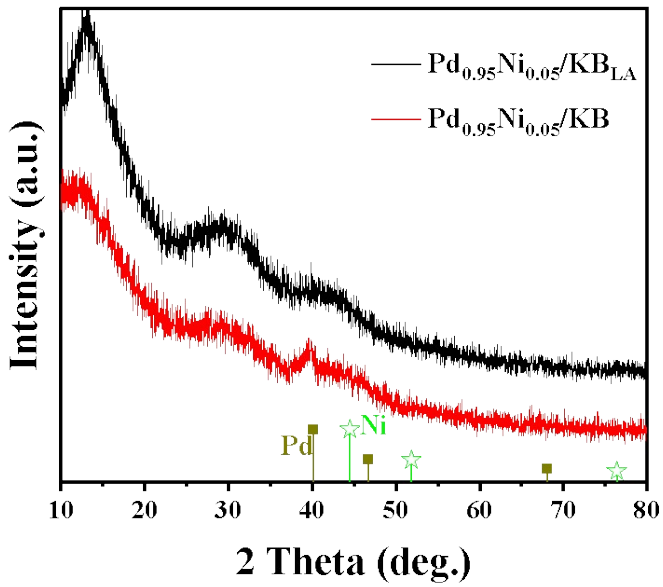

Figure S2. XRD patterns of $Pd_{0.95}Ni_{0.05}/KB_{LA}$ and $Pd_{0.95}Ni_{0.05}/KB$. The small peak at about 40° for $Pd_{0.95}Ni_{0.05}/KB$ suggested the larger particle size of metal NPs.

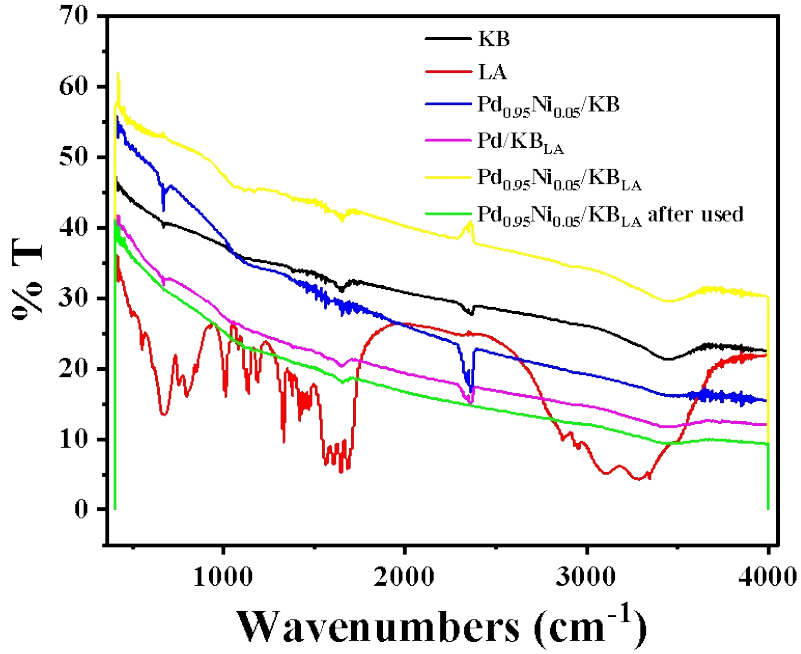

Figure S3. FT-IR spectra of KB, LA, $Pd_{0.95}Ni_{0.05}/KB$, Pd/KB_{LA}, $Pd_{0.95}Ni_{0.05}/KB_{LA}$ and $Pd_{0.95}Ni_{0.05}/KB_{LA}$ after used.

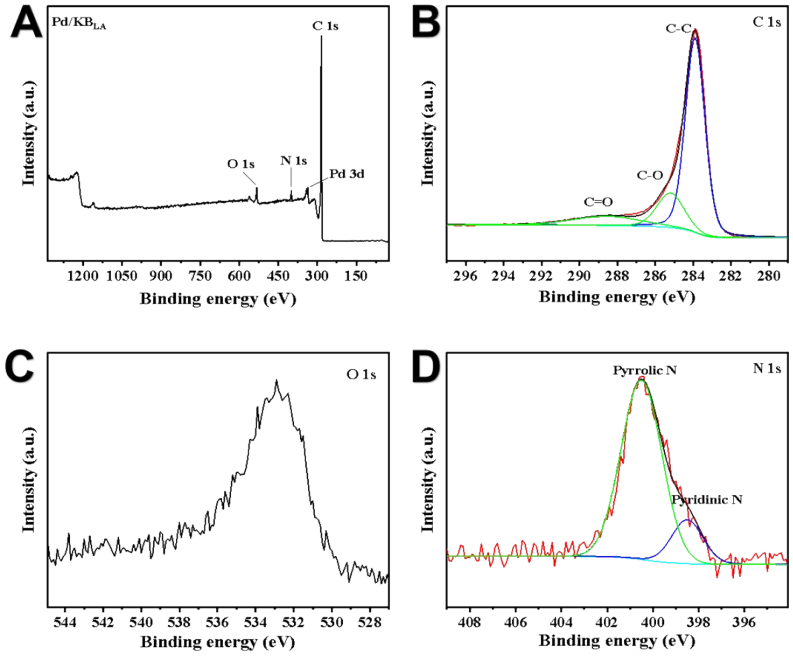

Figure S4. The XPS spectra of Pd/KB$_{LA}$: survey (A), O 1s (B), C 1s (C) and N 1s (D).

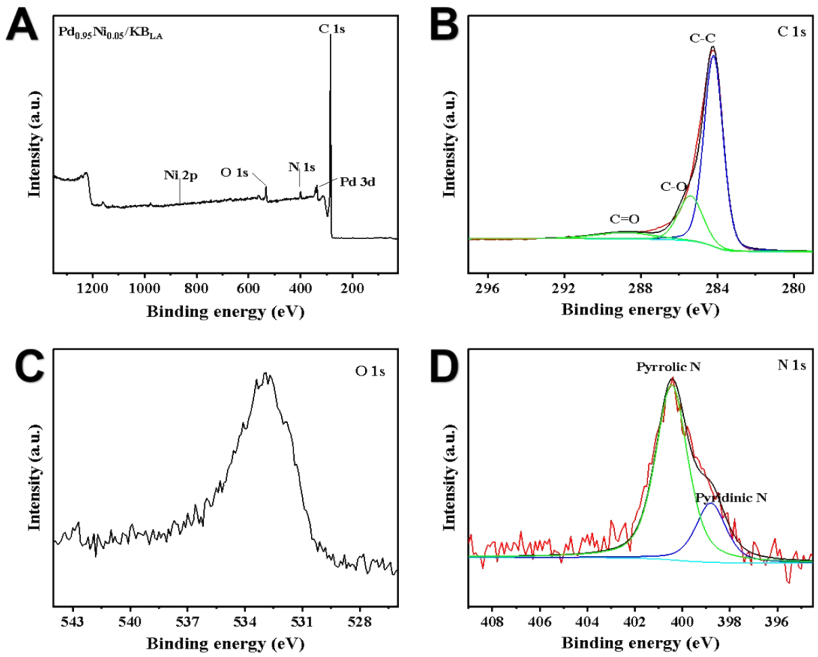

Figure S5. The XPS spectra of Pd$_{0.95}$Ni$_{0.05}$/KB$_{LA}$: survey (A), O 1s (B), C 1s (C) and N 1s (D).

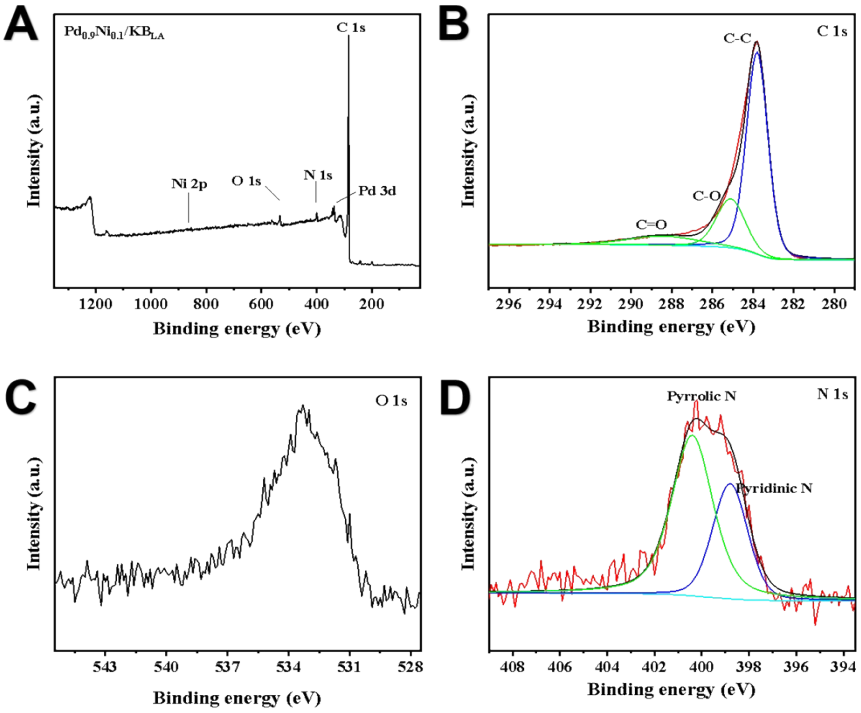

Figure S6. The XPS spectra of $Pd_{0.9}Ni_{0.1}/KB_{LA}$: survey (A), O 1s (B), C 1s (C) and N 1s (D).

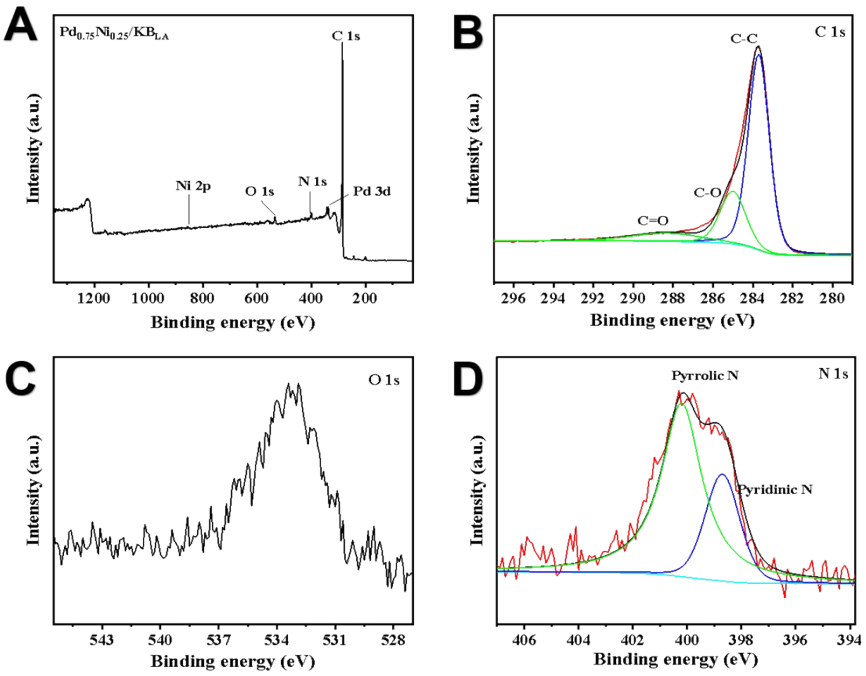

Figure S7. The XPS spectra of $Pd_{0.75}Ni_{0.25}/KB_{LA}$: survey (A), O 1s (B), C 1s (C) and N 1s (D).

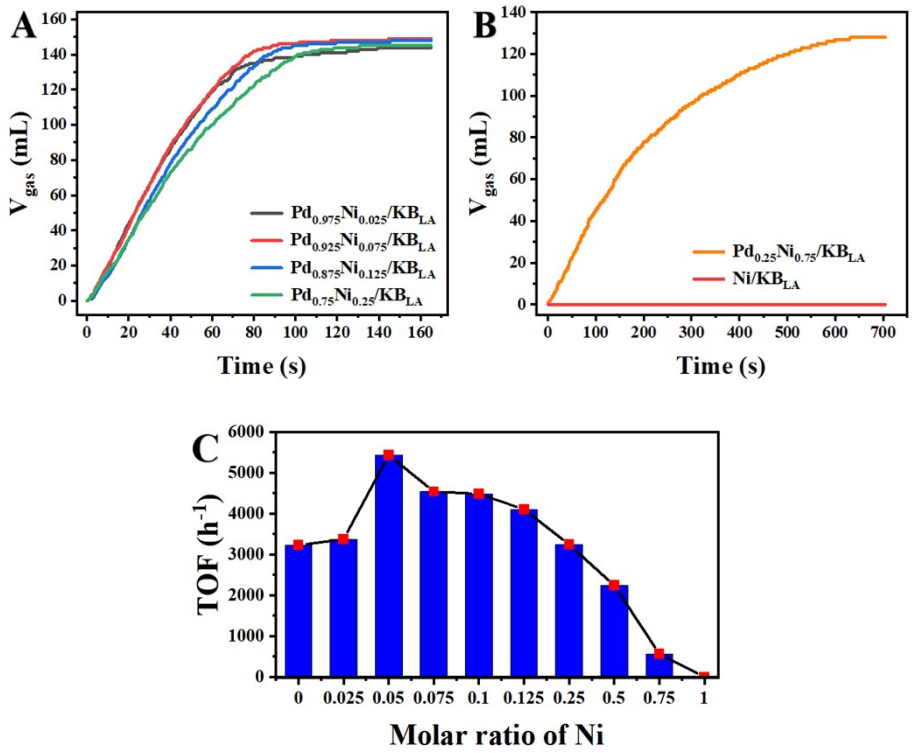

Figure S8. The volume of the generated gas (CO_2+H_2) *versus* time for the dehydrogenation of FA/SF solution over catalysts with different Pd/Ni ratios (A, B), and the corresponding TOF values (C) (T = 50 °C, [Pd+Ni] = 0.01 M, [FA] = 1.0 M and [SF] = 2.5 M in 3.0 mL aqueous dispersion).

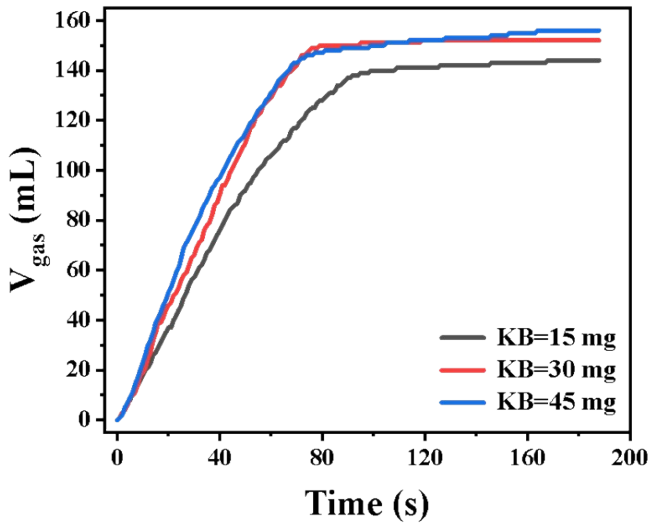

Figure S9. The volume of the generated gas (CO_2+H_2) *versus* time for the dehydrogenation of FA/SF solution over $Pd_{0.95}Ni_{0.05}/KB_{LA}$ with KB of different amounts as the support (T = 50 °C, [Pd+Ni] = 0.01 M, [FA] = 1.0 M and [SF] = 2.5 M in 3.0 mL aqueous dispersion).

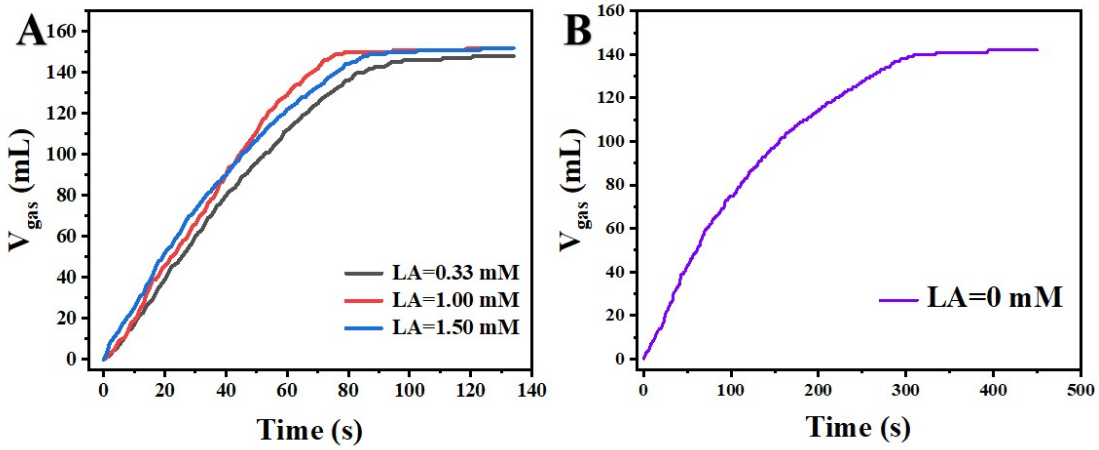

Figure S10. The volume of the generated gas (CO_2+H_2) *versus* time for the dehydrogenation of FA/SF solution over $Pd_{0.95}Ni_{0.05}/KB_{LA}$ prepared with LA of different amount (T = 50 °C, [Pd+Ni] = 0.01 M, [FA] = 1.0 M and [SF] = 2.5 M in 3.0 mL aqueous dispersion).

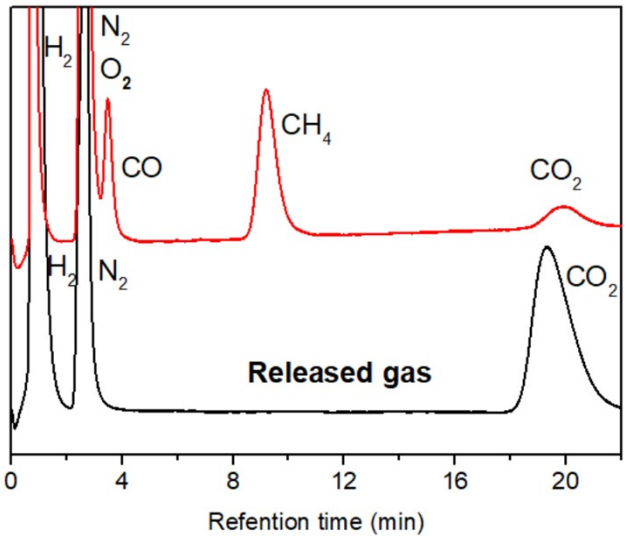

Figure S11. GC results of the released gas from the mixture of FA/SF over $Pd_{0.95}Ni_{0.05}/KB_{LA}$ ([Pd+Ni] = 0.01 M, [FA] = 1.0 M and [SF] = 2.5 M in 3.0 mL aqueous dispersion at 50 °C), showing the presence of only H_2 and CO_2.

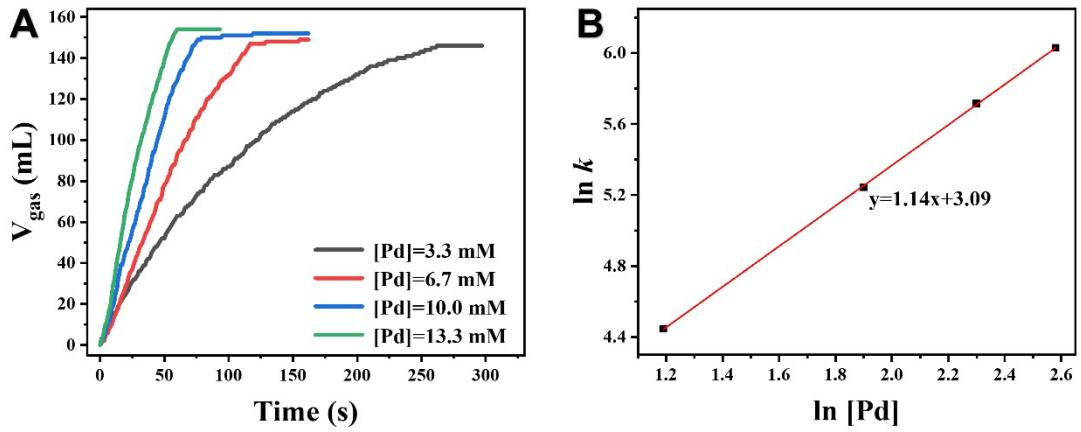

Figure S12. The volume of the generated gas (CO_2+H_2) *versus* time with different (Pd+Ni) concentrations (A), and the plot of the gas generation rate *versus* the (Pd+Ni) concentration (B) (both in logarithmic scale, y = 1.14x + 3.09, R^2 = 0.99) for the dehydrogenation of FA/SF solution over $Pd_{0.95}Ni_{0.05}/KB_{LA}$ (T = 50 °C, [FA] = 1.0 M and [SF] = 2.5 M in 3.0 mL aqueous dispersion).

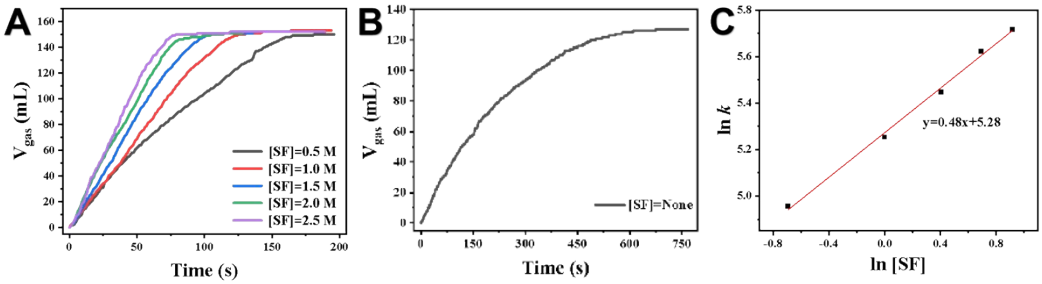

Figure S13. The volume of the generated gas (CO_2+H_2) *versus* time with different SF concentrations (A, B), and the plot of the gas generation rate *versus* the SF concentration (C) (both in logarithmic scale, y = 0.48x + 5.28, R^2 = 0.97) for the dehydrogenation of FA over $Pd_{0.95}Ni_{0.05}/KB_{LA}$ (T = 50 °C, [Pd+Ni] = 0.01 M and [FA] = 1.0 M in 3.0 mL aqueous dispersion).

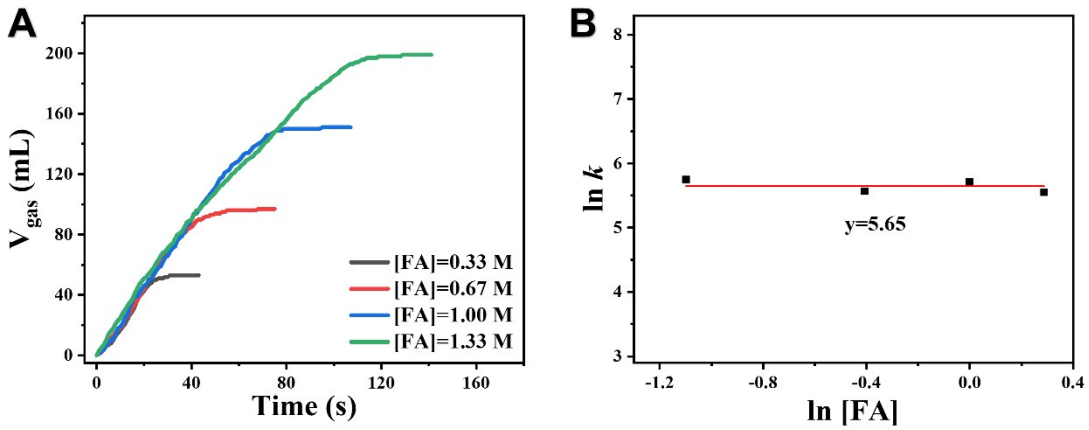

Figure S14. The volume of the generated gas (CO_2+H_2) *versus* time with different FA concentrations (A), and the plot of the gas generation rate *versus* the FA concentration (B) (both in logarithmic scale) for the dehydrogenation of FA over $Pd_{0.95}Ni_{0.05}/KB_{LA}$ (T = 50 °C, [Pd+Ni] = 0.01 M and [SF] = 2.5 M in 3.0 mL aqueous dispersion).

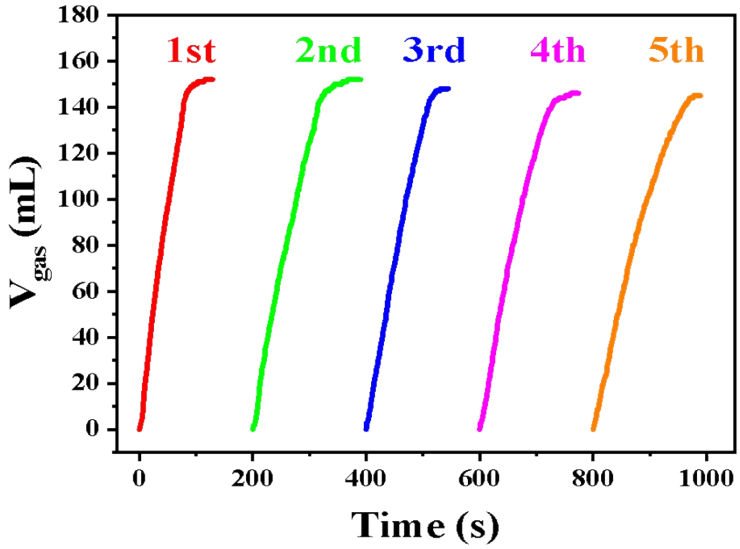

Figure S15. Durability test (5 cycles) for the dehydrogenation of FA/SF solution over $Pd_{0.95}Ni_{0.05}/KB_{LA}$ (T = 50 °C, [Pd+Ni] = 0.01 M, [FA] = 1.0 M and [SF] = 2.5 M in 3.0 mL aqueous dispersion).

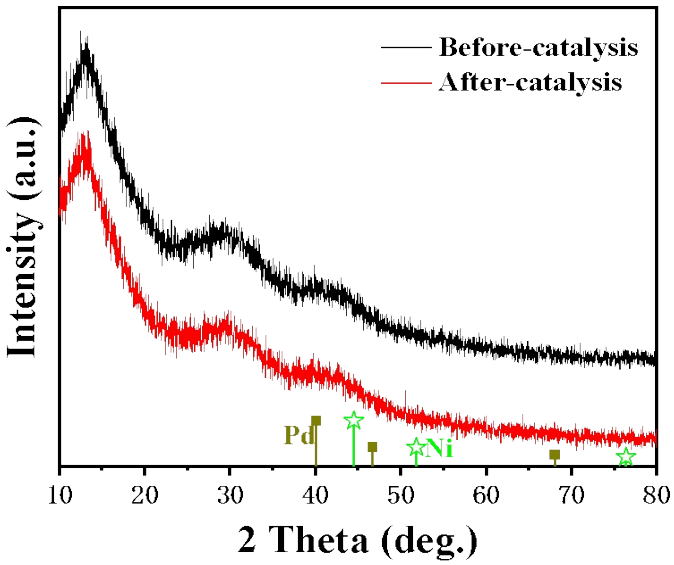

Figure S16. The XRD patterns of the $Pd_{0.95}Ni_{0.05}/KB_{LA}$ before and after catalysis.

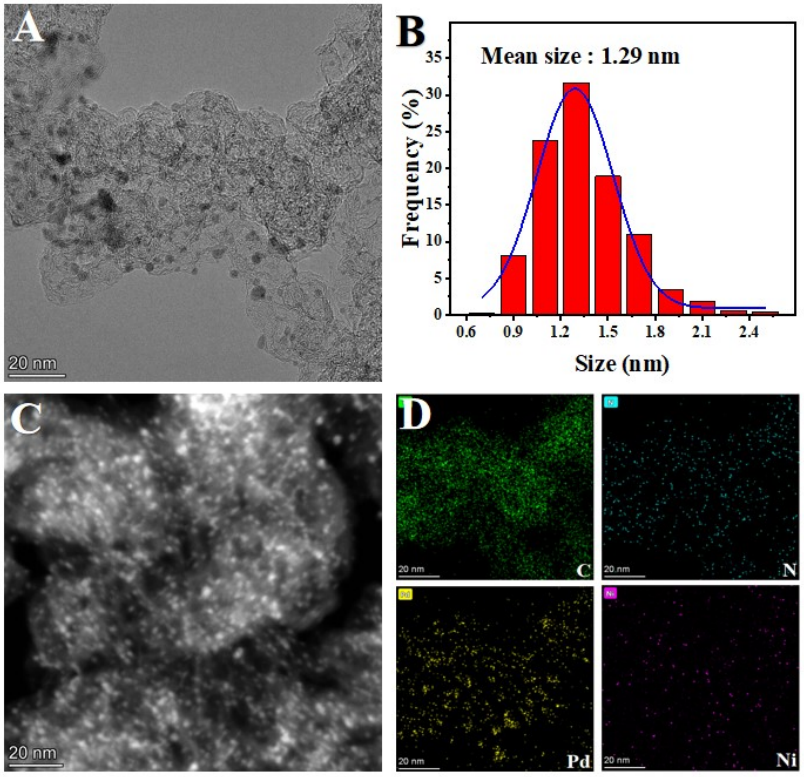

Figure S17. The TEM (A), particle size distribution (B), HADDF-STEM (C) and corresponding elemental mapping (D) images of $Pd_{0.95}Ni_{0.05}/KB_{LA}$ after used.

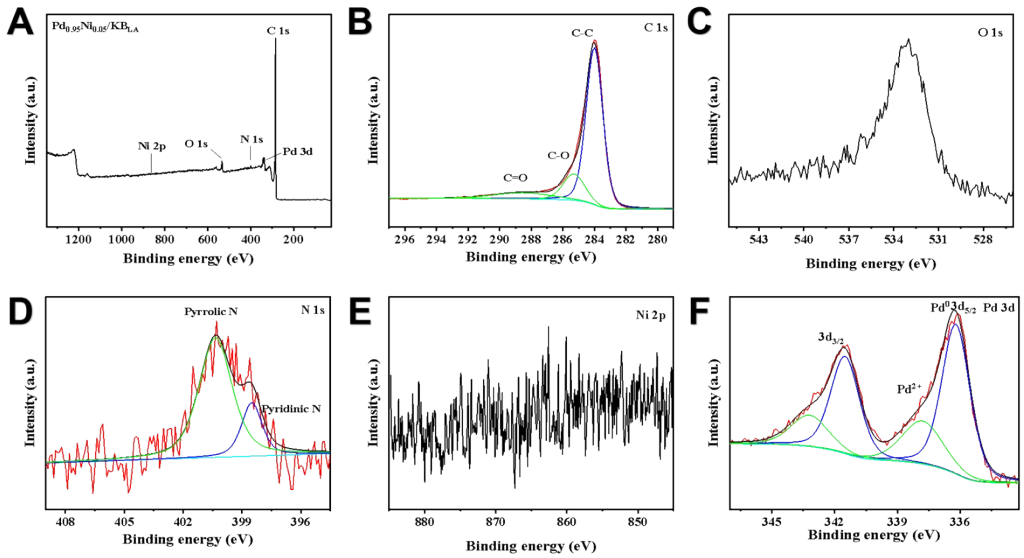

Figure S18. XPS spectra of $Pd_{0.95}Ni_{0.05}/KB_{LA}$ after used for FA dehydrogenation: survey (A), O 1s (B), C 1s (C), N 1s (D), Ni 2p (E) and Pd 3d (F).

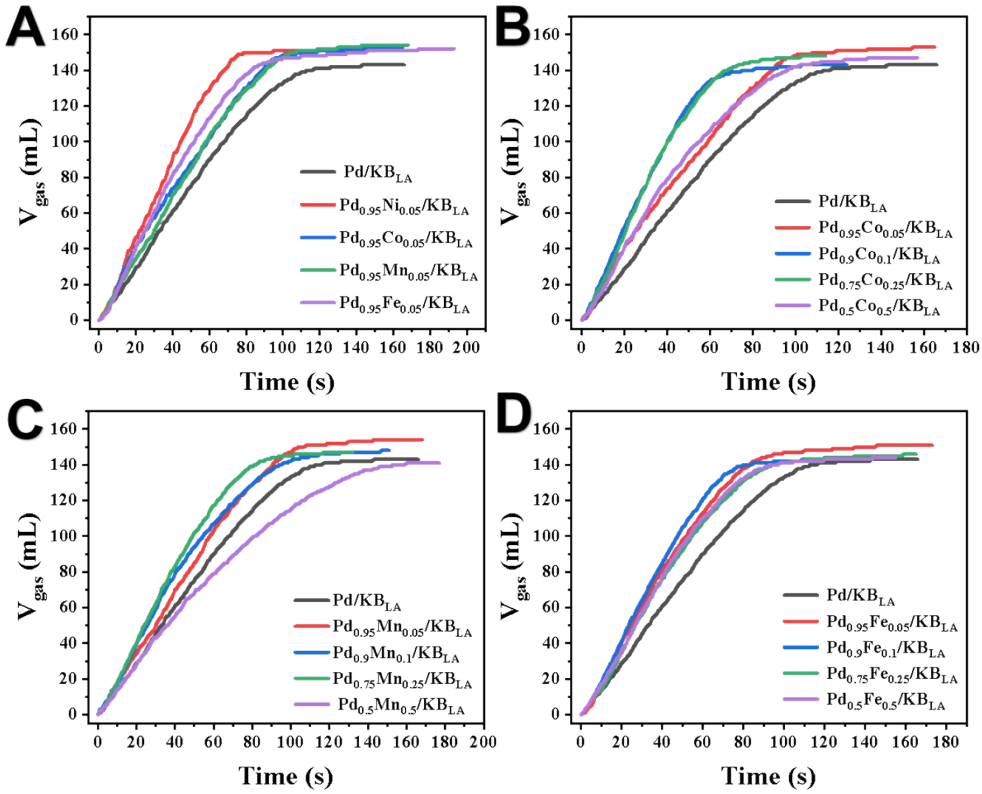

Figure S19. The volume of the generated gas (CO_2+H_2) *versus* time for the dehydrogenation of FA/SF solution over different catalysts. (A) Comparison of Pd-based catalysts with or without non-noble metals doping; (B-D) the effect of doping percentage for Co (B), Mn (C) and Fe (D) on catalytic performances (T = 50 °C, [Pd+M] = 0.01 M, [FA] = 1.0 M and [SF] = 2.5 M in 3.0 mL aqueous dispersion).

Table S1. BET surface areas and pore volumes for the synthesized samples.

Sample	Specific surface area / $m^2\ g^{-1}$	Pore volume / $cm^3\ g^{-1}$
KB	1322.99	1.35
$Pd_{0.95}Ni_{0.05}/KB_{LA}$	819.67	0.89

Table S2. Elemental contents of the samples.

Sample	C (wt%)	N (wt%)	H (wt%)
Pd/KB_{LA}	96.27	0.05	0.26
$Pd_{0.95}Ni_{0.05}/KB_{LA}$	79.61	4.74	1.91
$Pd_{0.95}Ni_{0.05}/KB_{LA}$ after used	81.80	2.81	1.71

Table S3. ICP results of $Pd_{0.95}Ni_{0.05}/KB_{LA}$ before and after used.

	Before use	After used
Pd (wt%)	8.15	8.38
Ni (wt%)	0.18	0.16

Table S4. Catalytic activities of latest heterogeneous catalysts for dehydrogenation of formic acid.

Catalyst	T (°C)	Solution	TOF (h^{-1})	E_a (kJ mol^{-1})	Ref.
Pd_1-$Ni(OH)_2$/PC	50	FA/SF	2008[a]*	47.5	1
PdNi-Pd/C	30	FA/SF	5654[a#]	24.44	2
Pd_1Ag_2/C (PVP/metal = 1)	75	FA/SF	855[a#]	---	3
Pd/Co@CN	30	FA/SF	1403[a]*	---	4
Ni@Pd NCs	25	FA	645[b]*	--	5
$Pd_{0.8}Au_{0.2}$/UiO-66-$(NH_2)_2$	50	FA/SF	3660[a#]	41.86	6
$Pd_{0.8}Au_{0.2}$/UiO-66-$(NH_2)_2$	25	FA/SF	980[a#]	41.86	6
$Pd_1Co_{0.7}$/g-C_3N_4	75	FA/SF	1193[a]*	--	7
$Pd_1Ni_{1.3}$/N-C	65	FA/SF	2195[a#]	27.6	8
PdNi@Pd/GNs-CB	25	FA/SF	577[b#]	--	9
$Pd_{0.9}Co_{0.1}/C_{650}$	60	FA/SF	8117[a#]	47.73	10
$Pd_{0.95}Ni_{0.05}/KB_{LA}$	30	FA/SF	**1522[a]***	**45.59**	**This work**
	40		**3187[a]***		
	50		**5432[a]***		
	60		**7714[a]***		

[a] TOF values calculated on total metal atoms.

[b] TOF values calculated on surface metal sites or active sites.

[#] Initial TOF values calculated on initial time or initial conversion of FA.

[*] TOF values calculated on the complete time of gas releasing.

1. Y. Dong, Q. Chen, C. Qiu, X. Ma, Y. Wang, T. Sun and G. Fan, *International Journal*

of Hydrogen Energy, 2020, **45**, 12849-12858.

2. N. Gao, R. Ma, X. Wang, Z. Jin, S. Hou, W. Xu, Q. Meng, J. Ge, C. Liu and W. Xing, *International Journal of Hydrogen Energy*, 2020, **45**, 17575-17582.

3. M. Navlani-García, K. Mori, A. Nozaki, Y. Kuwahara and H. Yamashita, *Industrial & Engineering Chemistry Research*, 2016, **55**, 7612-7620.

4. M. Yao, Y. Ye, H. Chen and X. Zhang, *Materials Letters*, 2020, **264**, 127308

5. Q. Tang, X. Zhou, J. Liu, M. Wu, H. Ji, Q. Wang, G. Li, H. Cong and Y. Qin, *International Journal of Hydrogen Energy*, 2022, **47**, 21745-21752.

6. R.-D. Ding, Y.-L. Li, F. Leng, M.-J. Jia, J.-H. Yu, X.-F. Hao and J.-Q. Xu, *ACS Applied Nano Materials*, 2021, **4**, 9790-9798.

7. M. Navlani-García, D. Salinas-Torres, K. Mori, Y. Kuwahara and H. Yamashita, *International Journal of Hydrogen Energy*, 2019, **44**, 28483-28493.

8. R. Tamarany, D. Y. Shin, S. Kang, H. Jeong, J. Kim, J. Kim, C. W. Yoon and D. H. Lim, *Phys Chem Chem Phys*, 2021, **23**, 11515-11527.

9. Y. L. Qin, J. Wang, F. Z. Meng, L. M. Wang and X. B. Zhang, *Chem Commun (Camb)*, 2013, **49**, 10028-10030.

10. J. Wu, J. Zuo, K. Liu, J. Lin and Z. Liu, *Catalysis Letters*, 2022, **170,** 1-10.